Analysis of the (0,0) band of the new [15.3]Ω=3/2 – $X\,^2\Pi_{3/2}$ electronic transition of PtF using intracavity laser spectroscopy

Caroline A. Welch[a], Jack C. Harms[a], James J. O'Brien[a], and Leah C. O'Brien[b,*]
[a]University of Missouri – St. Louis
[b]Southern Illinois University Edwardsville

Abstract:

A rotational analysis of the electronic transition of PtF occurring at 15,252 cm^{-1} was recorded and analyzed. This transition is identified as the (0,0) band of the [15.3]Ω=3/2 – $X\,^2\Pi_{3/2}$ electronic transition. The PtF molecules were produced in a current regulated RF discharge operating with 0.80 A applied to a Pt-lined copper hollow cathode in 0.50-1.25 Torr of 1-5% SF_6 in an Ar/He sputter gas mixture. The hollow cathode was placed within in the resonator cavity of a tunable DCM dye laser operating over the 14,500-16,500 cm^{-1} range, and path lengths of 0.2-2.0 km were utilized with the intracavity laser spectroscopy (ILS) method. The data were fit in PGOPHER using a polynomial energy level expression. Molecular constants for the excited state are presented. The nature of the new [15.3]Ω=3/2 state is discussed.

*corresponding author

Keywords: Platinum Fluoride, Electronic Spectroscopy, Molecular Radicals, Isotopologue structure

Introduction:

In the last two decades, various spectroscopic studies have investigated the electronic properties of platinum monofluoride, PtF. The original theoretical investigation into the electronic structure of PtF was performed by Liu and Franke [1] in 2002 who used the relativistic *ab initio* and density functional theory (DTF) methods to study various platinum containing diatomic radicals. Handler *et al.* [2] continued the exploration by analyzing the (1,0) and (0,0) vibrational bands of the [11.9]Ω=3/2 – $X\,^2\Pi_{3/2}$ transition of platinum monofluoride (PtF), recorded using intracavity laser spectroscopy (ILS). This research aided in the construction of a partially completed MO diagram of PtF and determination of molecular constants for the ground and excited states of those transitions. Shortly after, the permanent electric dipole moment and hyperfine interactions of ^{195}PtF for this same transition were analyzed by Qin *et al*. [3] using laser induced fluorescence (LIF) and Stark spectroscopy. Also in 2012, Okabayashi *et al.* [4] studied the ground $X\,^2\Pi_{3/2}$ state by microwave spectroscopy. In 2016, several electronic transitions of PtF were investigated by Ng *et al.* [5] using the technique of laser vaporization/reaction with free jet expansion and LIF. The four electronic transitions analyzed include the $[18.9]^2\Pi_{3/2} - X\,^2\Pi_{3/2}$, the $[18.9]\,^2\Pi_{3/2} - [0.04]^2\Delta_{5/2}$, the $[19.9]^2\Delta_{5/2} - X\,^2\Pi_{3/2}$ and the $[23.3]^2\Delta_{5/2} - X\,^2\Pi_{3/2}$ transitions. Molecular constants were determined for the excited states. The electronic landscape of PtF was expanded in 2019 by Harms *et al.* [6], who identified two new electronic states, where several vibrational bands of the [15.8+x]Ω=5/2 – $B\,^2\Delta_{5/2}$ electronic transition were discovered by ILS in the 14,500-16,500 cm^{-1} range. The observed transitions for the vibrational bands were fit to 16 mass-independent Dunham parameters. Theoretical calculations of the low-lying electronic states of PtF were performed by Zou *et al.* [7]. Their work presented potential energy curves for electronic states with T_e values up to 25,000 cm^{-1}, and associated molecular parameters and transition dipole moments to the 3 lowest-lying energy states were reported. Their calculations demonstrate that relativistic effects are prominent in defining the energetic landscape of the excited electronic states of PtF.

The focus of this paper is the rotational analysis of the (0,0) band of the new [15.3]Ω=3/2 –$X\,^2\Pi_{3/2}$ electronic transition.

Experimental Methods:

The ILS instrument used to perform these measurements has been described in detail previously [6,8]. Only an abbreviated description is provided. The PtF molecules were produced in the plasma discharge formed by applying RF current to a 50 mm long Pt-lined Cu hollow cathode. A variety of conditions were used to optimize signals due to the different band systems of PtF. Discharge currents ranged from 0.30 to 0.80 A, and the gas composition consisted of 1-5% SF_6 in either a mixture of Ar/He or just Ar, with total pressures ranging from 0.50 to 1.25 Torr. The hollow cathode was located in the resonator chamber of a Coherent Verdi^{TM} V-10 pumped DCM dye laser, enabling the enhancement by laser action of molecular absorption of species formed by the plasma. Generation times, t_g, ranging from 30-150 μsec for the 50 mm cathode and 1.1 m long resonator cavity resulted in effective pathlengths of 0.4 to 2.0 km. The dye laser was tuned over the 14,500-16,500 cm^{-1} range using an optical wedge in a rotatable mound attached to an xyz-translation stage.

The output of the dye laser was dispersed through a 2-m long echelle grating monochromator and onto a 1024-channel diode array detector. The spectral coverage at each monochromator position is ~7 cm^{-1} wide. Immediately after PtF data collection, iodine spectra from an extracavity cell were collected at each monochromator position for absolute wavenumber calibration using the digital data set provided by Salami and Ross [9]. The data were analyzed with PGOPHER [10].

Results & Discussion:

During the analysis of the [15.8+x]Ω=5/2 – $B\,^2\Delta_{5/2}$ electronic transition [6], a new electronic transition was observed at 15,252 cm^{-1} as shown in Figure 1 below. At first, only a single P-branch and a single R-branch are obvious in the spectrum. On the low-energy side of this spectrum, it is clear to see that the high-J lines of the new transition are obscured by the (0,1) vibrational band of the [15.8+x]Ω=5/2 – $B\,^2\Delta_{5/2}$ electronic transition, and all line positions < 15,198 cm^{-1} are entirely masked by this transition. After measuring the line positions of the new transition, we used the molecular constants determined by microwave spectroscopy [4] to calculate Δ_2F values [11] and we were able to conclude that this spectrum did originate from the $X\,^2\Pi_{3/2}$ state of PtF. Based on the branch structure and clear rotational lines, we also concluded that this spectrum showed the (0,0) band of an electronic transition with an Ω=3/2 excited state.

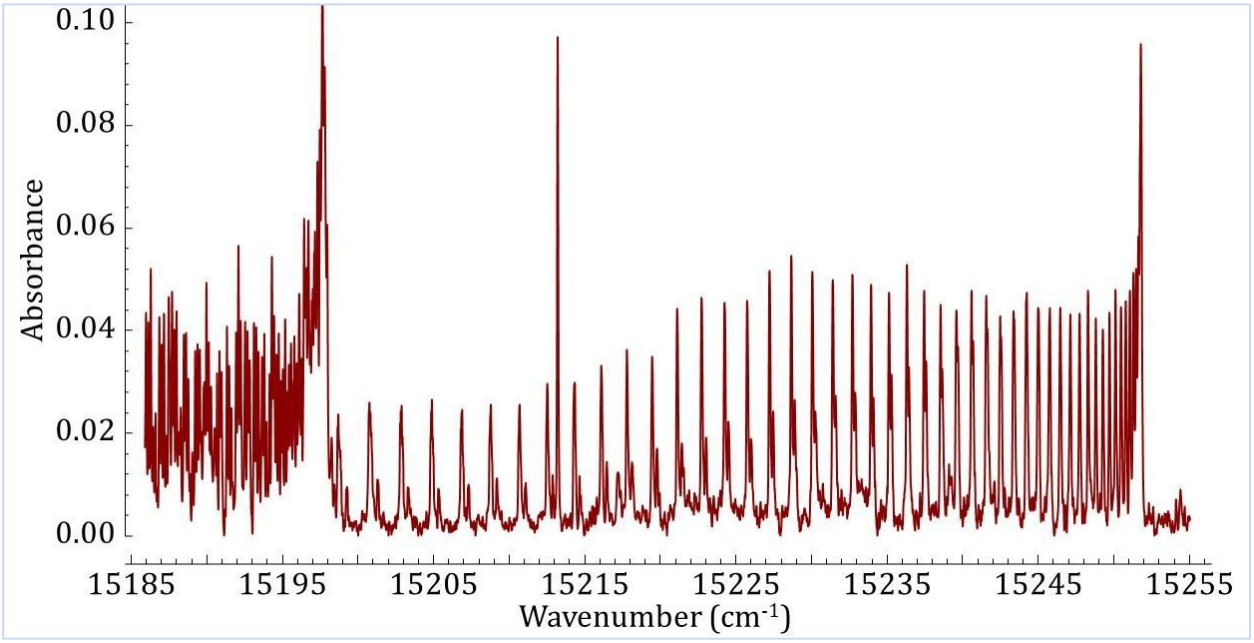

Figure 1. The newly observed spectrum of PtF with bandhead at 15,252 cm^{-1}. The (0,1) band of the [15.8+x]Ω=5/2 – $B\,^2\Delta_{5/2}$ electronic transition (left side) overpowers the new transition; an atomic line is observed at ~15,213 cm^{-1}.

Upon addition of the ground-state Λ-doubling parameters from Tanimoto [4], it became clear that the Λ-doubling in the R-branch was fully resolved. Unfortunately, the R_f lines actually were blended with the $P_{e,f}$ lines, as shown in Figure 2.

One interesting spectral observation was the linewidth, measured up to 0.15 cm^{-1}. This is much wider than the typical ILS instrument-limited line width of 0.035 cm^{-1}, even considering the blending of the R_f and $P_{e,f}$ lines. To account for the line widths, separate PtF isotopologues were added to the PtF manifold in PGOPHER [10]. All peaks were re-measured using 3 line positions to account for the 3 major isotopologues, ^{194}PtF (32%), ^{195}PtF (33%), and ^{196}PtF (26%). Using a reasonable guess for the isotopologue separations based on the linewidth, the individual isotopologue peaks were estimated as a symmetric triplet. For each observed peak, the lower energy line position was assigned to ^{194}PtF, while the higher energy component line position was assigned to ^{196}PtF, consistent with the expected origin shifts for a red-degraded (0,0) band of an electronic transition. Line positions for ^{198}PtF (7%) also were eventually added. Several attempts at line position measurements were necessary to procure a spectral simulation that resembled the features of our raw spectrum. Ultimately, a very satisfactory fit was obtained, as shown in Figure 3. Additionally, this approach was successful at explaining the observed line widths.

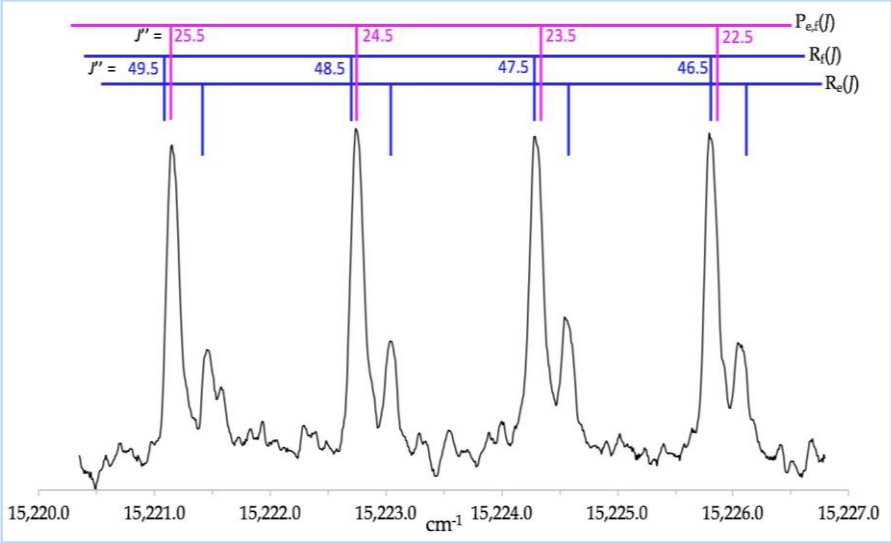

Figure 2. A portion of the spectrum from 15220 to 15227 cm^{-1} where the two P-branch and two R-branch components are indicated, recorded by ILS. Λ-doubling increases with J, and these components begin to be resolved at J~30.5

All line positions were fit in PGOPHER **[10]**. The ground and excited state rotational energy levels were constrained to a Hund's case (c) energy level expression for Ω=3/2 electronic states, where the large spin-orbit coupling of Pt leads to the mixing of the theoretical ΛS states of PtF. This was accomplished by choosing the 3/2 component of a $^2\Pi$ state with a $\mathbf{R^2}$ Hamiltonian: from the 'Constants' window, choose S=0.5, Lambda=Π, and OmegaSelect=1.5. The effective Hamiltonian is then a polynomial of form:

$$E= B[J(J+1)+S(S+1)–\Omega^2–\Sigma^2] – D[J(J+1)+S(S+1)–\Omega^2–\Sigma^2]^2 + H[J(J+1)+S(S+1)–\Omega^2–\Sigma^2]^3$$
$$\mp \tfrac{1}{2}q_D(J–1/2)(J+1/2)(J+3/2)$$

The line positions from Okabayashi *et al.* **[4]** were included in our data set yielding nearly identical molecular constants to their values except for Λ-doubling parameters; in previous work, we had noted that q and q_J values corresponded to $-q_D$ and $-q_H$ values in PGOPHER, respectively **[12]**.

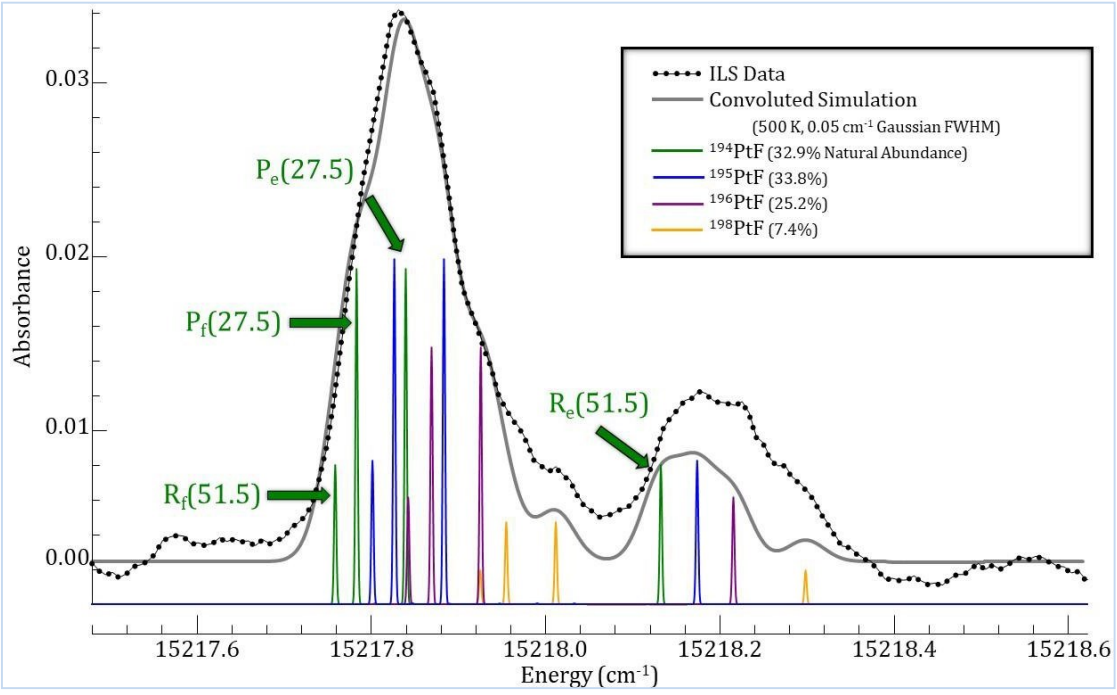

Figure 3. Lambda doubling components of each of the four major isotopologues of PtF (^{194}PtF, ^{195}PtF, ^{196}PtF, and ^{198}PtF) for the transitions corresponding to P(23.5) and R(47.5).

For the [15.3]Ω=3/2 excited state, 'constraint' statements were added to the PGOPHER input file to ensure that the B′, D′, and H′ values for each isotopologue would be consistent with calculated isotopologue relationships: $B^i=B\rho^2$, $D^i=D\rho^4$, $H^i=H\rho^6$, where $\rho^i=(\mu/\mu^i)^{½}$ and *i* is an index for the isotope of interest [11]. In our work, we assumed these relationships are exact for v=0 (i.e., the excited state r_0 value is the same for all isotopologues): however, these are exact only for r_e within the Born-Oppenheimer approximation. The excited state origin frequencies (T_0 values) of the 4 isotopologues were fit independently, though clearly they were influenced by the estimated triplet spacings used for the line position measurements of the 3 main isotopologues. Since the isotopologue positions are not resolved, the fitted errors in these parameters do not represent the real error bars of the T_0 values. The simulation in Figures 3 and 4 is an excellent reproduction of the rotational features of this electronic transition, therefore confidence is placed on the excited state molecular constants.

A total of 541 line positions were included in the fit. Line positions, assignments and residuals are shown in Table 1. The RMS residuals associated with all line positions is found to be 0.004 cm^{-1}. Note that for ^{196}PtF and ^{198}PtF only the P_e and R_e branches were measured: the P_f and R_f lines were deemed to be impossible to measure and unimportant to the fit. The molecular parameters for the new [15.3]Ω=3/2 electronic state are given in Table 2. Note that the observed Λ-doubling in the spectrum can be attributed entirely to the ground state q_D value in this analysis. The r_0 bond length for the excited state is also included in Table 2, with r_0 = 1.9505 Å.

Using the excellent calculations of Zou and Suo [7], it is interesting to compare and correlate their findings with the experimental data and results. Potential energy curves of the low-lying electronic states of PtF provided by Zou and Suo [7] estimate that both the fifth and sixth calculated Ω=3/2 electronic states occur near 15,300 cm^{-1}. The experimental excited state value of B′=0.2560 cm^{-1} agrees more favorably with B=0.2568 cm^{-1} of the fifth Ω=3/2 state than with B=0.2618 cm^{-1} for the sixth Ω=3/2 state. Thus, we assigned our excited [15.3]Ω=3/2 state as their fifth Ω=3/2 state, i.e., their (5)3/2 state.

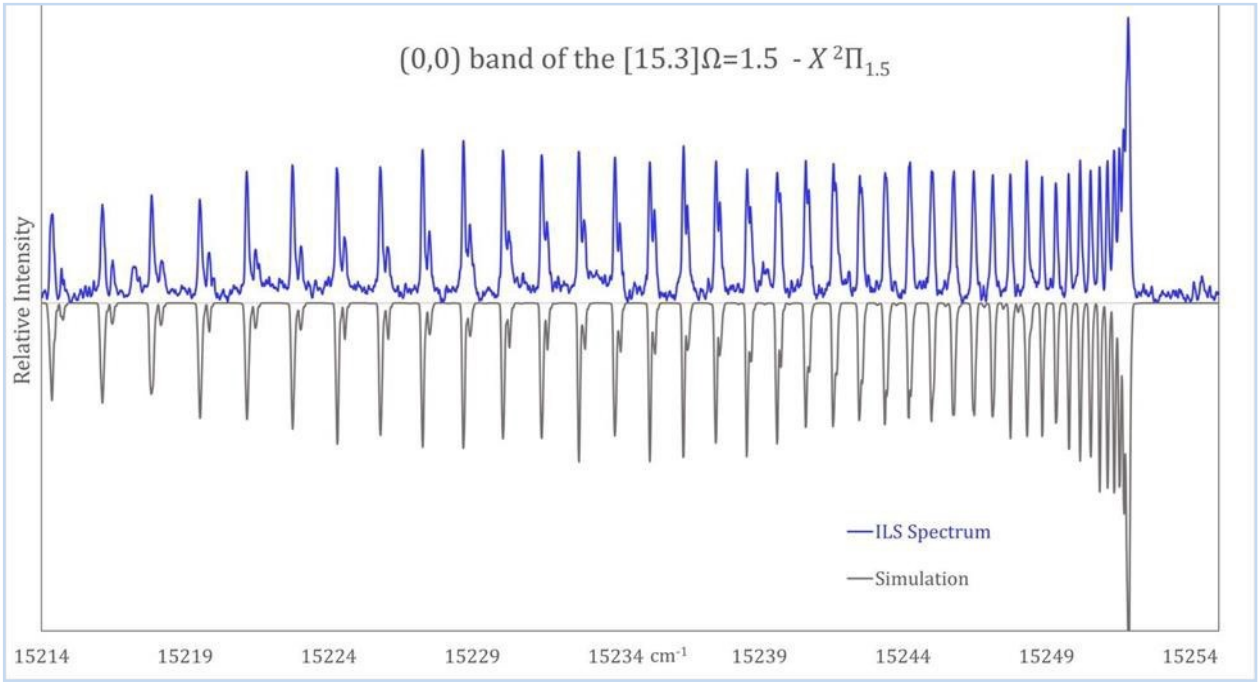

Figure 4. The final spectral fit of the [15.3]Ω=3/2 – $X\,^2\Pi_{3/2}$ electronic transition of PtF optimized in PGOPHER presented with the experimental spectrum on the top (blue) and PGOPHER simulation (grey) with T=500 K and Gaussian line width (FWHM) of 0.05 cm^{-1}.

It should be possible to use the excited state origin shifts to garner information about the excited state vibrational frequency. Zou and Suo [7] predict the vibrational frequency for their (5)3/2 state as ω_e=603.9 cm^{-1}. Using the isotopologue relationship for vibration with $\omega_e^i = \rho\omega_e$ [11], the predicted isotopologue origin shifts are significantly underestimated, ~0.015 cm^{-1} *c.f.* an observed shift of ~0.03 cm^{-1}. However, the potential energy curves for Ω=3/2 states in their paper [7] show an avoided crossing between the (5)3/2 and (6)3/2 states at approximately 1.86 Å. Thus, this perturbation may account for some of the discrepancy. Additionally, recall our previous statements that the reported errors for T_0 are not representative of their values, i.e., our measurements of the isotopologue line positions have systematic errors based on the user's choice 'symmetric-triplet' positions and perceived linewidth.

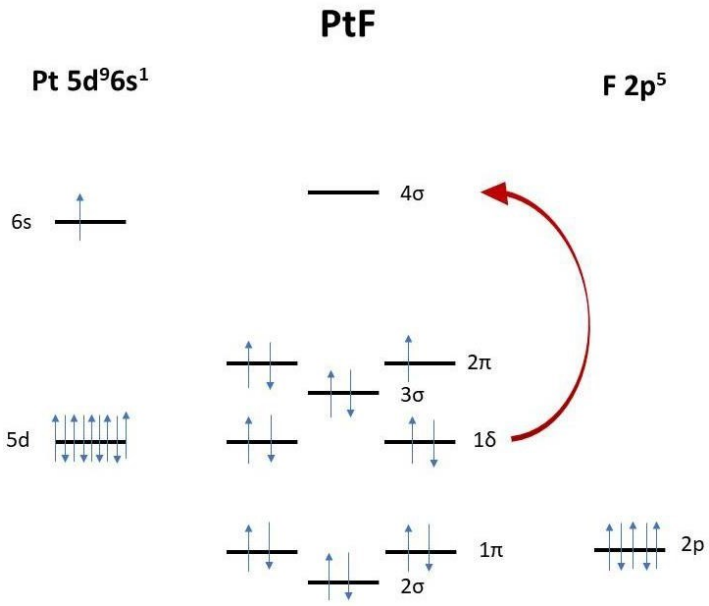

Figure 5. Molecular orbital diagram for PtF. The electron configuration for the ground state is shown. The red arrow represents the likely electronic excited to produce electron configuration for the [15.3]Ω=3/2 excited state.

A simplistic molecular orbital diagram for PtF is shown in Figure 5, which shows a qualitative picture of ionic bonding. The electron configuration shown in the figure is $\delta^4 1\sigma^2\pi^3 2\sigma^0$, consistent with the $X\,^2\Pi_{3/2}$ ground state. The ΛS components of the (5)3/2 state from Zou and Suo [7] are reported to be the (I)$^4\Pi$(26%) + (I) $^4\Delta$(26%) + (II)$^2\Delta$(13%) + (II)$^2\Pi$(12%) states. Moreover, the primary $^4\Pi$ and $^4\Delta$ parents are reported to be associated with the second ^{4}F atomic state of Pt^+ [7]. According to Moore's tables [13] for PtII (Pt^+), the second ^{4}F state has an atomic configuration of $5d^8[^3F]6s^1$, and the ^{3}F atomic term can only arise from unpaired electrons on the $d_{m=\pm2}$ and $d_{m=\pm1}$ orbitals that correlate to the metal-centered δ and π molecular orbitals shown below. Thus, not only do the primary $^4\Pi$ and $^4\Delta$ parents represent spin-forbidden transitions, but also this electronic transition would be an orbital-forbidden excitation from a δ-orbital to a σ-orbital. This helps explain why the transition dipole moment is so weak, since a non-zero transition dipole moment can occur only through the minor ΛS components of the (5)3/2 electronic state presented above. Indeed, the calculated transition dipole moment is quite small, $|R^2_{tot}|$= 0.035 a.u. [7].

The lack of Λ-doubling in the excited state also warrants consideration. Based on the ΛS components of the (5)3/2 state given above, the primary components of this state are the $^4\Pi_{3/2}$ and $^4\Delta_{3/2}$ states [7]. Neither of these states would be expected to have large Λ-doubling parameters.

Conclusions:

A rotational analysis of the electronic transition of PtF occurring at 15,252 cm^{-1} was recorded and analyzed. Molecular parameters for the [15.3]Ω=3/2 excited state were obtained. This transition is identified as the (0,0) band of the [15.3]Ω=3/2 – X $^2\Pi_{3/2}$ electronic transition. The data were fit using PGOPHER [10] as described above. The pronounced isotopologue structure follows isotope relationships and accounts for the excessive line widths of the observed peaks. The new state corresponds to the (5)3/2 state predicted by Zou and Suo [7].

Acknowledgements

This work was supported by the National Science Foundation, Grant Nos. CHE-1955773 (JOB) and CHE-1955776 (LOB).

Supplementary Materials

The Supplementary Materials include the PGOPHER files used in the fit, including the PGOPHER configuration, the spectrum overlay, and the input and output files from the fit.

References:

[1] W. Liu, R. Franke, J. Comput. Chem. 23 (2003) 564-575.

[2] K.G. Handler, R.A. Harris, L.C. O'Brien, J.J. O'Brien, J. Mol. Spec. 265 (2011) 39-46.

[3] C. Qin, R. Zhuang, F. Wang, T.C. Steimle, J. Chem. Phys. 137 (2012) 054309.

[4] T. Okabayashi, T. Kurahara, E.Y. Okabayashi, M. Tanimoto, J. Chem. Phys. 136 (2012) 174311.

[5] K.F. Ng, A.M. Southam. A.S.-C. Cheung, J. Mol. Spec. 328 (2016) 32-36.

[6] J.C. Harms, L.C. O'Brien, J.J. O'Brien, J. Mol. Spec. 355 (2019) 101-108.

[7] W. Zou, B. Suo, J. Phys. Chem. A 120 (2016) 6357-6370.

[8] J.C. Harms, L.C. O'Brien, J.J. O'Brien, J. Chem. Phys. 148 (2018) 204306.

[9] H. Salami and A. J. Ross, J. Mol. Spec. 223 (2005) 157-159.

[10] PGOPHER, A Program for Simulating Rotational, Vibrational and Electronic Spectra, C. M. Western, JQSRT, 186 (2017) 221-242.

[11] G. Herzberg, Spectra of Diatomic Molecules. Krieger Publishing (1989).

[12] J.C. Harms, J. Wu, S. Mian, L.C. O'Brien, and J.J. O'Brien, J. Mol. Spec. 359 (2019) 6-15.

[13] C. Moore, Atomic Energy Levels, V3, NBS 35 (1958).

TABLES:

Table 1a. Assignments, Line Positions, and Residuals for ^{194}PtF, in cm^{-1}.

J''	P_e	O-C	P_f	O-C	R_e	O-C	R_f	O-C
4.5	15245.6852	0.0016	15245.6852	0.0019				
5.5	15244.9392	0.0012	15244.9392	0.0017				
6.5	15244.1529	0.0028	15244.1529	0.0037				
7.5	15243.3174	-0.0024	15243.3174	-0.0011				
8.5	15242.4437	-0.0034	15242.4437	-0.0015				
9.5	15241.5295	-0.0026	15241.5295	0.0000				
10.5	15240.5759	0.0012	15240.5676	-0.0037				
11.5	15239.5734	-0.0017	15239.5734	0.0027				
12.5	15238.5320	-0.0011	15238.5237	-0.0038				
13.5	15237.4504	0.0015	15237.4422	0.0003	15251.7881	0.0040		
14.5	15236.3214	-0.0010	15236.3132	-0.0005	15251.6802	-0.0005		
15.5	15235.1535	-0.0001	15235.1453	0.0022	15251.5309	-0.0039	15251.5226	-0.0017
16.5	15233.9390	-0.0037	15233.9311	0.0011	15251.3485	0.0019	15251.3319	-0.0021
17.5	15232.6900	0.0005	15232.6734	-0.0011	15251.1164	0.0005	15251.0998	-0.0012
18.5	15231.3940	-0.0001	15231.3775	0.0011	15250.8430	0.0001	15250.8264	0.0011
19.5	15230.0517	-0.0048	15230.0353	-0.0006	15250.5283	0.0009	15250.5034	-0.0034
20.5	15228.6719	-0.0049	15228.6555	0.0026	15250.1724	0.0028	15250.1476	0.0019
21.5	15227.2547	-0.0002	15227.2302	0.0027	15249.7671	-0.0022	15249.7420	0.0004
22.5	15225.7916	0.0007	15225.7586	-0.0010	15249.3291	0.0024	15249.2957	0.0003
23.5	15224.2849	0.0000	15224.2521	0.0029	15248.8419	0.0001	15248.8089	0.0028
24.5	15222.7416	0.0049	15222.6924	-0.0040	15248.3139	-0.0006	15248.2727	-0.0014
25.5	15221.1454	-0.0011	15221.1044	0.0033	15247.7453	0.0005	15247.7041	0.0047
26.5	15219.5173	0.0031	15219.4678	0.0045	15247.1338	0.0010	15247.0815	-0.0004
27.5	15217.8395	-0.0005	15217.7814	-0.0018	15246.4821	0.0036	15246.4240	0.0023
28.5	15216.1250	0.0013	15216.0594	-0.0011	15245.7848	0.0029	15245.7184	-0.0003
29.5	15214.3657	0.0002	15214.2974	0.0019	15245.0439	0.0009	15244.9723	-0.0007
30.5	15212.5692	0.0038	15212.4869	-0.0012	15244.2604	-0.0014	15244.1860	0.0015
31.5	15210.7231	-0.0002	15210.6396	0.0014	15243.4421	0.0037	15243.3513	-0.0020
32.5	15208.8409	0.0015	15208.7472	0.0013	15242.5756	0.0029	15242.4767	-0.0026
33.5	15206.9101	-0.0035	15206.8118	0.0005	15241.6612	-0.0036	15241.5624	-0.0001
34.5	15204.9492	0.0033	15204.8345	0.0002	15240.7128	-0.0019	15240.6005	-0.0025
35.5	15202.9380	0.0015	15202.8129	-0.0020	15239.7231	0.0007	15239.5990	-0.0018
36.5	15200.8872	0.0019	15200.7492	-0.0040	15238.6868	-0.0012	15238.5568	0.0010
37.5	15198.7918	-0.0006	15198.6422	-0.0049	15237.6118	0.0004	15237.4670	-0.0010
38.5					15236.4893	-0.0034	15236.3379	0.0003
39.5					15235.3343	0.0024	15235.1617	-0.0027
40.5					15234.1273	-0.0018		
41.5					15232.8884	0.0042		

42.5					15231.6001	0.0027		
43.5					15230.2656	-0.0030		
44.5					15228.8968	-0.0011		
45.5					15227.4861	0.0008		
46.5					15226.0307	-0.0001		
47.5					15224.5316	-0.0030		
48.5					15222.9957	-0.0009		
49.5					15221.4146	-0.0022		
50.5					15219.7974	0.0020		
51.5					15218.1353	0.0029		
52.5					15216.4274	-0.0005		
53.5					15214.6763	-0.0055		
54.5					15212.8965	0.0022		
55.5					15211.0659	0.0004		
56.5					15209.1913	-0.0040		
57.5					15207.2835	-0.0004		
58.5					15205.3263	-0.0050		
59.5					15203.3397	0.0021		
60.5					15201.3015	-0.0013		
61.5					15199.2252	-0.0020		

Table 1b. Assignments, Line Positions, and Residuals for ^{195}PtF, in cm^{-1}.

J''	P_e	O-C	P_f	O-C	R_e	O-C	R_f	O-C
4.5								
5.5	15245.7184	-0.0002	15245.7184	-0.0003				
6.5	15244.9723	-0.0002	15244.9723	0.0000				
7.5	15244.1860	0.0017	15244.186	0.0022				
8.5	15243.3513	-0.0026	15243.3513	-0.0017				
9.5	15242.4767	-0.0046	15242.4767	-0.0031				
10.5	15241.5624	-0.0040	15241.5624	-0.0019				
11.5	15240.6087	-0.0005	15240.6087	0.0024				
12.5	15239.6072	-0.0026	15239.6072	0.0013				
13.5	15238.5651	-0.0031	15238.5651	0.0021				
14.5	15237.4834	-0.0009	15237.4752	-0.0025	15251.8130	0.0005	15251.8047	-0.0013
15.5	15236.3544	-0.0037	15236.3462	-0.0038	15251.7134	0.0044	15251.7009	0.0000
16.5	15235.1864	-0.0033	15235.1781	-0.0017	15251.5641	0.0009	15251.5558	0.0026
17.5	15233.9815	0.0023	15233.9643	-0.0028	15251.3734	-0.0015	15251.3651	0.0022
18.5	15232.7230	-0.0034	15232.7065	-0.0055	15251.1420	-0.0022	15251.1330	0.0032
19.5	15231.4352	0.0037	15231.4104	-0.0041	15250.8678	-0.0034	15250.8512	-0.0030
20.5	15230.0928	-0.0016	15230.0764	0.0019	15250.5531	-0.0027	15250.5365	0.0007

21.5	15228.7129	-0.0023	15228.6965	0.0045	15250.1978	-0.0002	15250.1724	-0.0024
22.5	15227.2956	0.0018	15227.2711	0.0040	15249.8002	0.0024	15249.7671	-0.0040
23.5	15225.8328	0.0024	15225.7998	0.0000	15249.3548	-0.0005	15249.3208	-0.0039
24.5	15224.326	0.0011	15224.2849	-0.0051	15248.8749	0.0045	15248.8337	-0.0018
25.5	15222.7743	-0.0030	15222.7385	0.0007	15248.3469	0.0037	15248.3057	0.0020
26.5	15221.1863	-0.0014	15221.1421	-0.0010	15247.7782	0.0045	15247.7288	-0.0003
27.5	15219.5585	0.0024	15219.5104	0.0044	15247.1602	-0.0017	15247.1114	-0.0004
28.5	15217.8806	-0.0018	15217.8231	-0.0034	15246.5071	-0.0007	15246.4489	-0.0029
29.5	15216.1659	-0.0009	15216.1086	0.0040	15245.8096	-0.0017	15245.7477	-0.0014
30.5	15214.4148	0.0055	15214.3425	0.0022	15245.0717	-0.0010	15244.2147	-0.0007
31.5	15212.6104	0.0006	15212.5363	0.0027	15244.2935	0.0018	15243.3843	-0.0002
32.5	15210.7707	0.0022	15210.6863	0.0019	15243.4671	-0.0014	15242.5073	-0.0035
33.5	15208.8891	0.0038	15208.7963	0.0033	15242.6015	-0.0016	15241.5895	-0.0049
34.5	15206.9581	-0.0021	15206.8606	0.0015	15241.6947	-0.0008	15240.6311	-0.0041
35.5	15204.9902	-0.0032	15204.8802	-0.0027	15240.7484	0.0027	15239.6344	0.0011
36.5	15202.9870	0.0023	15202.8629	-0.0014	15239.7572	0.0035	15238.5878	-0.0009
37.5	15200.9359	0.0015	15200.7982	-0.0052	15238.7221	0.0025	15237.4981	-0.0033
38.5	15198.8425	0.0002	15198.7024	0.0022	15237.6484	0.0050	15236.3684	-0.0029
39.5					15236.5233	-0.0018	15235.1946	-0.0040
40.5					15235.3613	-0.0034	15233.9815	-0.0016
41.5					15234.1620	-0.0003		
42.5					15232.9150	-0.0029		
43.5					15231.6331	0.0017		
44.5					15230.3080	0.0049		
45.5					15228.9344	0.0016		
46.5					15227.5175	-0.0032		
47.5					15226.0713	0.0045		
48.5					15224.5728	0.0018		
49.5					15223.0374	0.0039		
50.5					15221.4562	0.0018		
51.5					15219.8386	0.0051		
52.5					15218.1764	0.0053		
53.5					15216.4690	0.0019		
54.5					15214.7254	0.0037		
55.5					15212.9345	-0.0003		
56.5					15211.1094	0.0029		
57.5					15209.2366	-0.0004		
58.5					15207.3329	0.0067		
59.5					15205.3746	0.0003		
60.5					15203.3786	-0.0026		
61.5					15201.3465	-0.0007		

	^{196}PtF				^{198}PtF			
J''	P_e	O-C	R_e	O-C	P_e	O-C	R_e	O-C
4.5	15245.7516	0.0057						
5.5	15245.0055	0.0045						
6.5	15244.2190	0.0053						
7.5	15243.3873	0.0031						
8.5	15242.5179	0.0056						
9.5	15241.5953	-0.0028						
10.5	15240.6416	0.0000						
11.5	15239.6414	-0.0014						
12.5	15238.5981	-0.0036						
13.5	15237.5180	-0.0005						
14.5	15236.3956	0.0027						
15.5	15235.2221	-0.0031						
16.5	15234.0124	-0.0029						
17.5	15232.7644	0.0012	15251.1744	0.0015			15251.2241	-0.0049
18.5	15231.4682	-0.0007	15250.9001	0.0010			15250.9589	0.0025
19.5	15230.1357	0.0032	15250.5862	0.0014	15230.2080	0.0006	15250.6442	0.0028
20.5	15228.7539	-0.0001	15250.2303	0.0031	15228.8277	-0.0023	15250.2882	0.0041
21.5	15227.3365	0.0031	15249.8250	-0.0023	15227.4102	-0.0004	15249.8829	-0.0016
22.5	15225.8740	0.0033	15249.3869	0.0018	15225.9482	-0.0010	15249.4448	0.0023
23.5	15224.3679	0.0020	15248.8997	-0.0008	15224.4412	-0.0045	15248.9601	0.0018
24.5	15222.8153	-0.0038	15248.3724	-0.0012	15222.8990	-0.0012	15248.4376	0.0058
25.5	15221.2280	-0.0022	15247.8029	-0.0014	15221.3089	-0.0038	15247.8606	-0.0025
26.5	15219.5997	0.0003	15247.1936	0.0008	15219.6847	0.0015	15247.2513	-0.0007
27.5	15217.9310	0.0044	15246.5403	0.0013	15218.0120	0.0002	15246.5985	-0.0003
28.5	15216.2154	0.0036	15245.8428	-0.0002	15216.2970	-0.0015	15245.9035	0.0003
29.5	15214.4571	0.0020	15245.1055	0.0008	15214.5374	-0.0059	15245.1629	-0.0026
30.5	15212.6604	0.0039	15244.3266	0.0025	15212.7401	-0.0061	15244.3845	-0.0011
31.5	15210.8139	-0.0021	15243.4999	-0.0014	15210.9019	-0.0054	15243.5688	0.0053
32.5	15208.9346	0.0009	15242.6333	-0.0031	15209.0278	0.0012	15242.7005	0.0013
33.5	15207.0069	-0.0027	15241.727	-0.0022	15207.1032	-0.0009	15241.7951	0.0024
34.5	15205.0410	-0.0026	15240.7812	0.0014	15205.1377	-0.0021	15240.8413	-0.0029
35.5	15203.0359	0.0000	15239.7903	0.0019	15203.1279	-0.0059	15239.8556	0.0021
36.5	15200.9858	-0.0007	15238.7557	0.0009	15201.0857	-0.0005	15238.8213	0.0006
37.5	15198.8950	-0.0004	15237.6815	0.0025	15198.9997	0.0029	15237.7475	0.0016
38.5			15236.5608	-0.0005			15236.6324	0.0034
39.5			15235.4001	-0.0013			15235.4741	0.0040
40.5			15234.1969	-0.0027			15234.2667	-0.0026
41.5			15232.9546	-0.0011			15233.0289	0.0024
42.5			15231.6661	-0.0038			15231.7448	0.0031
43.5			15230.3396	-0.0026			15230.4137	-0.0014

44.5	15228.9681	-0.0045	15229.0445	-0.0021
45.5	15227.5575	-0.0036	15227.6312	-0.0051
46.5	15226.1050	-0.0029	15226.1874	0.0031
47.5	15224.6139	0.0011	15224.6916	0.0011
48.5	15223.0729	-0.0032	15223.1598	0.0048
49.5	15221.4970	-0.0006	15221.5826	0.0047
50.5	15219.8750	-0.0026	15219.9564	-0.0028
51.5	15218.2196	0.0037	15218.2997	0.0007
52.5	15216.5101	-0.0027	15216.5943	-0.0029
53.5	15214.7744	0.0063	15214.8524	-0.0017
54.5	15212.9789	-0.0032	15213.0759	0.0064
55.5	15211.1561	0.0014	15211.2464	0.0027
56.5	15209.2894	0.0034	15209.3740	-0.0026
57.5	15207.3730	-0.0032	15207.4699	0.0015
58.5	15205.4247	-0.0005	15205.520	0.0010
59.5	15203.4318	-0.0013	15203.5331	0.0044
60.5	15201.3990	-0.0010	15201.4982	0.0008
61.5	15199.3234	-0.0027	15199.4215	-0.0037

Table 2. Molecular Constants for the [15.3]Ω=3/2 state, in cm^{-1} except where noted.

	Origin	B_0	$D_0 \times 10^7$	$H_0 \times 10^{12}$	r_0, Å
^{194}PtF [a]	15248.47645(43)	0.25608143	2.45495	2.416	1.9505
^{195}PtF	15248.50679(43)	0.25596400(106)	2.45270(739)	2.413(137)	1.9505
^{196}PtF [a]	15248.53624(49)	0.25584801	2.45048	2.410	1.9505
^{198}PtF [a]	15248.59516(70)	0.25561923	2.44610	2.403	1.9505

[a] B_0, D_0, and H_0 values constrained to isotopic relationship based on ^{195}PtF.

Conflict of Interest Statement, June 18, 2021

Analysis of the (0,0) band of the new [15.3]Ω=3/2 –$X\,^2\Pi_{3/2}$ transition using intracavity laser spectroscopy

Caroline A. Welch,[a] Jack C. Harms,[a] James J. O'Brien,[a] and Leah C. O'Brien[b]
[a]University of Missouri – St. Louis
[b]Southern Illinois University Edwardsville

The authors have no conflict of interest regarding the research and data that are contained in this manuscript.

Author Credit Statement

Analysis of the (0,0) band of the new [15.3]Ω=3/2 – $^2X\,\Pi_{3/2}$ electronic transition of PtF using intracavity laser spectroscopy

Caroline A. Welch, Jack C. Harms, James J. O'Brien, and Leah C. O'Brien

Caroline A. Welch: Formal analysis, Writing - Original Draft, Visualization

Jack C. Harms: Methodology, Software, Validation, Investigation, Data Curation, Writing - Review & Editing,

James J. O'Brien: Conceptualization, Software, Validation, Resources, Data Curation, Visualization, Writing - Review & Editing, Supervision, Funding acquisition

Leah C. O'Brien: Conceptualization, Methodology, Formal analysis, Resources, Writing - Review & Editing, Visualization, Project administration, Funding acquisition

PtF pgopher file

PtF Input file

SM_Final Fit